Med Ultrason 2025, Vol. 27, no. 1, 104-116

A case of primary lymphoma of the right atrium was misdiagnosed by ultrasound

Wenjun Chen, Yanbing Hu, Dongmei Lv

Department of Ultrasound Medicine, The Second Hospital of Jilin University, Changchun, Jilin, China

To the Editor,

A 61-year-old female patient was admitted due to a 5-year history of palpitations, with aggravated palpitations and fatigue for 2 weeks. The patient had no symptoms of chest pain, low-grade fever, or weight loss. Physical examination revealed no superficial lymphadenopathy. The ECG showed a heart rate of 91 beats/min, with first-degree atrioventricular block. Laboratory investigations showed a decreased lymphocyte percentage (18.9%). Transthoracic echocardiography (TTE) revealed a 70.3×30.8 mm solid isoechoic mass in the right atrium (fig 1a), suggestive of myxoma. Computed tomography angiography (CTA) revealed patchy low-density filling defects within the left atrium, right atrium, and right ventricle. Subsequently, the patient underwent cardiac mass removal (fig 1b). Intraoperative transesophageal echocardiography (TEE) showed a solid mass in the right atrium, which invaded the left atrial side (fig 1c). The postoperative pathological immunohistochemical analysis of the mass (fig 1d) revealed CD20 (+), Ki67 (85% positive), PAX-5 (+), Bcl-2 (90% positive), MUM1 (+), CD2 (-), CD3 (-), CD10 (-), Bcl-6 (-). Pathological findings confirmed diffuse large B-cell lymphoma (DLBCL), non-germinal center type (fig 1e). The clinical recommendation was for subsequent radiotherapy and chemotherapy.

Primary cardiac lymphoma (PCL) is an extremely rare malignant tumor of the myocardium, with diffuse large B-cell lymphoma (DLBCL) being the most common histopathological type [1]. Cardiac lymphoma can affect any cardiac compartment but predominantly affects the right atrium, followed by the pericardium and the left cardiac chambers [2]. In our case, the patient presented without the typical symptoms of lymphoma.

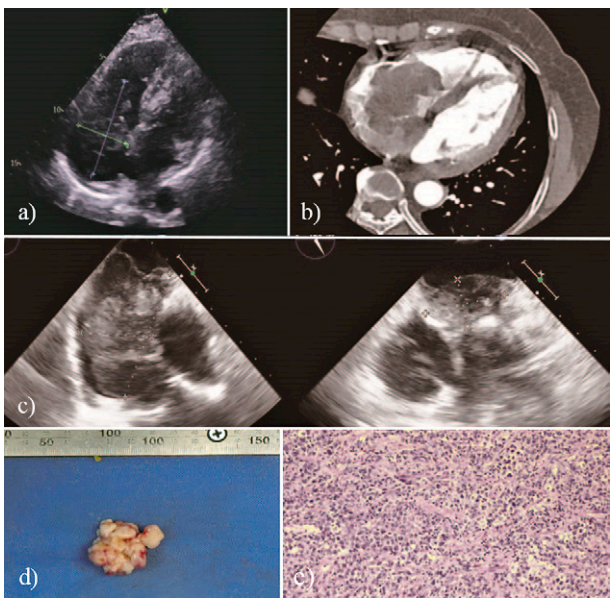

Fig 1. a) Transthoracic echocardiography, four-chamber section showed a 70.3×30.8 mm solid isoechoic mass in the right atrium; b) Computed tomography angiography showed low density in the right atrium, left atrium and right ventricle; c) Intraoperative transesophageal echocardiography showed a solid mass in the right atrium invading the left atrium; d) The surgically removed mass was histopathologically confirmed as a diffuse large B-cell lymphoma (e).

DLBCL is a malignant tumor, but the manifestations of its lesions can easily be misdiagnosed as benign tumors by imaging examinations. DLBCL imaging findings are nonspecific, and histopathological examination is the definitive method for diagnosis. Learning and understanding the clinical presentations, typical ultrasound manifestations, and multimodal imaging results of PCL can broaden the diagnostic ideas and avoid misdiagnosis of such diseases.

Received 20.01.2025 Accepted 05.02.2025
Med Ultrason
2025, Vol. 27, No 1, 104-105, DOI: 10.11152/mu-4472,
Corresponding author: Dongmei Lv
Department of Ultrasound Medicine,
The Second Hospital of Jilin University,
130022 Changchun, Jilin, China
Phone: 18088665681
E-mail: lvdongmei68@sina.com

References

1. Chia AXF, Zhao Z, Lim SL. Primary cardiac lymphoma. BMJ Case Rep 2019;12:e230468.
2. Farhoud N, Farhoud H, Deutsch JM. Primary Cardiac Lymphoma in a Young and Immunocompetent Patient Diagnosed by Percutaneous Transvenous Biopsy. Am J Cardiol 2023;201:139-141.

One case of rare urethral leiomyoma diagnosed by ultrasound

Di Zhang*, Xiaoxue Wang*, Lihua Huang, Xu Guo, Guangming Jin

** the authors share the first authorship*

Department of Medical Ultrasound, Yanbian University Hospital, Yanji, Jilin, China

To the Editor,

A 49-year-old female patient came to our hospital with the chief complaint of "a mass in the external orifice of the urethra for 10 years and dysuria for 1 year". Physical examination revealed multiple palpable masses at the external orifice of the urethra from 12 to 3 o 'clock, the largest being about 2.5x3 cm, hard in texture, with little mobility, no tenderness, and no fluid exudation during extrusion. Transvaginal ultrasound showed the presence of multiple solid, echogenic and inhomogeneous structures around the vagina, with partial fusion conglobation, the largest size being about 6.4x4.4 cm. The boundary between the vagina and the solid masses was irregular and unclear and rich blood flow signal was detected in and around the masses (resistive index of 0.89). The conclusion was of multiple solid masses in the pelvic cavity of unknown nature. After admission, the patient underwent resection of paraurethral gland lesion under general anesthesia. During the operation, more than ten irregularly shaped masses were removed, the largest being of 7x3x2 cm. Postoperative pathological results showed urethral leiomyoma (fig 1).

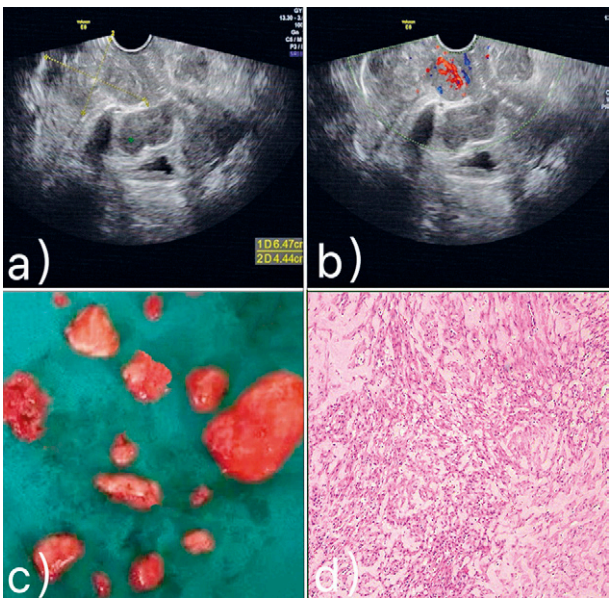

Fig 1. a) Transvaginal Color Doppler ultrasound showed that there were multiple solid hypoechoic masses around the vagina, some of which fused into clusters. The largest one was about 6.4x4.4 cm, with unclear boundary with vagina, irregular shape, and uneven internal echo; b) Abundant blood flow signals were observed in and around the mass, RI: 0.89; c) More than 10 irregularly shaped masses were removed during the operation, the largest being 7x3x2 cm; d) Postoperative pathological results showed urethral leiomyoma.

Urethral leiomyoma (UL) is a rare benign mesenchymal tumor originating from the smooth muscle of the urethra. It is a deep soft tissue leiomyoma, which can grow in any part of the urethra, and is commonly found in the proximal urethra. The disease can occur in both men and women, but the incidence is higher in women, with an average age of about 41 years [1]. UL usually has no clinical symptoms when it is small. When the mass gradually increases, the main symptom is a painless mass protruding from the external orifice of the urethra, which can cause recurrent urinary tract infection, dysuria, urinary

Received 08.07.2024 Accepted 03.09.2024
Med Ultrason
2025, Vol. 27, No 1, 105-106, DOI: 10.11152/mu-4473,
Corresponding author: Guangming Jin
Department of Medical Ultrasound,
Yanbian University Hospital,
#1327 Juzi Street,
Yanji 133000, China
Phone: +86-433-2660056
E-mail: jgm920@sina.com

retention and other complications. Complete surgical resection is the only effective treatment for this disease [2]. The prognosis is good, but recurrence may occur. Ultrasonography showed that UL was a hypoechoic mass around the urethra without obvious specific signs. This disease needs to be differentiated from bladder tumor. There is usually a clear boundary between UL and the bladder, but a bladder tumor would grow from the bladder wall to the bladder cavity, the surface is not smooth, and calcifications are common. In female patients, differentiation from uterine subserosal fibroids and broad ligament fibroids is needed. Understanding the typical symptoms and signs of UL, combined with the ultrasonographic findings, is the key to the diagnosis of UL.

Acknowledgement: This work was funded by Natural Science Foundation of Jilin Province (YDZJ202201 ZYTS204)

References

1. Wu S, Min Z, Wu L, et al. A urethral leiomyoma presenting with dysuria: A rare case report. Medicine 2024:103:e37893.
2. Misal M, Yi J. Exploring the Retropubic Space: Resection of Urethral Leiomyoma. J Minim Invas Gyn 2020; 27:S89.

"Sono-vision" of muscle contractions during peripheral magnetic stimulation

Wei-Ting Wu[1,2], Ke-Vin Chang[1,2,3], Kamal Mezian[4], Vincenzo Ricci[5], Levent Özçakar[6]

[1]Department of Physical Medicine and Rehabilitation, National Taiwan University Hospital, Bei-Hu Branch, Taipei, Taiwan, [2]Department of Physical Medicine and Rehabilitation, National Taiwan University College of Medicine, Taipei, Taiwan, [3]Center for Regional Anesthesia and Pain Medicine, Wang-Fang Hospital, Taipei Medical University, Taipei, Taiwan, [4]Department of Rehabilitation Medicine, Charles University, First Faculty of Medicine and General University Hospital in Prague, Prague, Czech Republic, [5]Physical and Rehabilitation Medicine Unit, Luigi Sacco University Hospital, ASST Fatebenefratelli-Sacco, Milano, Italy, [6]Department of Physical and Rehabilitation Medicine, Hacettepe University Medical School, Ankara, Turkey

To the Editor,

Ultrasound is an effective tool for assessing muscle echotexture and providing real-time visualization of muscle contractions [1]. Various physical modalities, including transcutaneous electrical stimulation (TES) and peripheral magnetic stimulation (PMS), have been developed to facilitate muscle activation. However, TES is limited by the resistance of skin and subcutaneous tissues, which restricts the delivery of high electrical currents needed to activate deep muscles. It also causes significant discomfort in this sense. On the contrary, PMS utilizes Faraday's law of electromagnetic induction to convert magnetic energy into electrical currents, enabling the stimulation of large-caliber nerves and inducing contractions of the innervated muscles [2]. A recent study has highlighted the potential benefits of combining PMS with ultrasound-guided dextrose prolotherapy in the management of low back pain [3]. Herewith, possibly due to the modulation of proprioceptive afferents through muscle contraction, there is limited evidence on whether PMS alone reliably induces muscle contraction.

The TESLA Stym® device (Iskra Medical d.o.o., Slovenia) was used in this study. The applicator was positioned over the ipsilateral lumbar region of a volunteer in the prone position. Stimulation intensity was set at 50% of the device's maximum output (2.5 Tesla/sec), with a frequency range of 5-20 Hz. An ultrasound transducer was placed over the posterior thigh to visualize the hamstring muscles. Synchronized hamstring contractions

Received 04.12.2024 Accepted 03.02.2025
Med Ultrason
2025, Vol. 27, No 1, 106-107, DOI: 10.11152/mu-4474,
Corresponding author: Ke-Vin Chang
Department of Physical Medicine and Rehabilitation,
National Taiwan University Hospital,
Bei-Hu Branch,
No. 87, Nei-Jiang Rd.,
Wan-Hwa District, Taipei 108, Taiwan
E-mail: kvchang011@gmail.com

Fig 1. Peripheral magnetic stimulation was applied to the ipsilateral lumbar region, with the ultrasound transducer positioned in the axial plane at the proximal posterior thigh (a), gluteal (b) and lower lumbar (c) regions. SEMIT, semitendinosus muscle; BICF, biceps femoris muscle; asterisk, sciatic nerve; ADM, adductor magnus muscle; GMAX, gluteus maximus muscle; PIR, piriformis muscle; MUL, multifidus muscle; LON, longissimus thoracis muscle; ILC, iliocostalis lumborum muscle; black arrows, radiating echo gradient.

were observed following PMS activation, indicating successful stimulation of the sciatic nerve (fig 1a, Video 1).

When the transducer was moved to the gluteal region along the piriformis muscle, simultaneous contractions of the gluteus maximus and piriformis muscles - characterized by several radiating echo gradients - were observed (fig 1b). Interestingly, when the transducer was positioned over the lumbar region, just distal to the applicator, contractions of the longissimus thoracis and iliocostalis lumborum muscles – characterized by two radiating echo gradients – were more pronounced as compared to those of the multifidus (fig 1c). Since the multifidus muscle spans only two vertebral levels, the medial branches of the posterior rami of the spinal nerves corresponding to the multifidus were possibly not fully encompassed by the magnetic field of the applicator. This report demonstrates the capability of PMS to activate the lumbosacral plexus and induce synchronized muscle contractions downstream of the stimulation site. Accordingly, our findings suggest that PMS may be a novel tool for restoring muscle endurance and strength in patients with low back pain.

Acknowledgment: This study was funded by the National Taiwan University Hospital, Bei-Hu Branch; Ministry of Science and Technology, Taiwan (MOST 106-2314-B-002-180-MY3 and MOST 109-2314-B-002-114-MY3) and National Science and Technology, Taiwan (NSTC 112-2314-B-002-134, NSTC 113-2314-B-002-208-MY2 and NSTC 113-2314-B-002-209-MY2).

References

1. Chang KV, Wu WT, Özçakar L. Ultrasound imaging and rehabilitation of muscle disorders: Part 1. Traumatic injuries. Am J Phys Med Rehabil 2019;98:1133-1141.
2. Kanjanapanang N, Chang KV. Peripheral magnetic stimulation. In StatPearls; Treasure island (FL) 2024.
3. Wu WT, Chang KV, Özçakar L. Integrating ultrasound-guided multifidus injections with repeated peripheral magnetic stimulation for low back pain: A feasibility study. J Pain Res 2024;17:2873-2880.

A case of solitary fibrous tumor of the breast

Fangtong Teng, Yue You, Hongyan Cui

Department of Ultrasound, The Second Affiliated Hospital of Dalian Medical University, Dalian, China

Received 14.11.2024 Accepted 12.12.2024
Med Ultrason
2025, Vol. 27, No 1, 107-108, DOI: 10.11152/mu-4482,
Corresponding author: Hongyan Cui
The Second Affiliated Hospital of
Dalian Medical University,
Dalian, 116027, China
E-mail:cuihongyan2024@163.com
E-mail: jgm920@sina.com

To the Editor,

A 38-year-old female noticed a palpable mass in the right breast for 2 weeks. Ultrasound (US) examination revealed a hypoechoic lesion at 10 o'clock position of the right breast glandular layer, measuring 7.7x5.0x3.7 cm, with regular shape, clear boundaries, smooth edges, visible blood flow signals within and around and soft

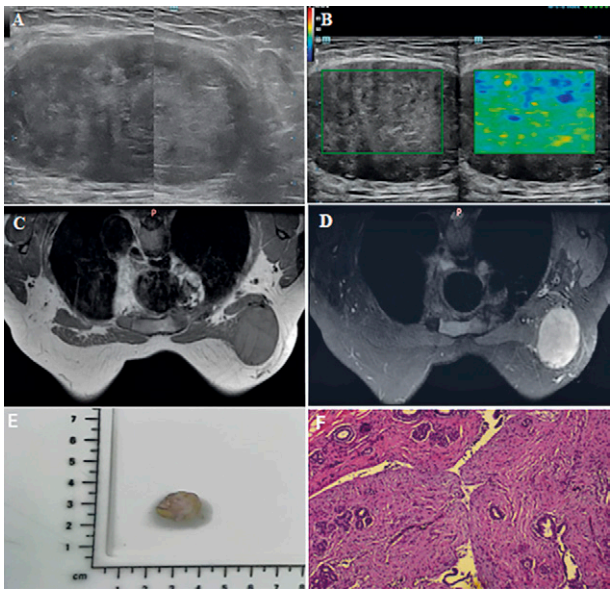

Fig 1. (A) US scan showed regular shape, clear boundaries, smooth edges; (B)Shear wave elastography showed a soft elasticity; (C-D) MRI showed T1W1 low-to-intermediate signal, T2W1 slightly high signal, high signal on diffusion-weighted imaging (DWI), regular morphology, smooth margins, and visible vascular flow voids; (E-F) Pathology showed the tumor borders are locally unclear, the fibrous interstitium has a certain heterogeneity, and the leaf-like structure can be seen in the foci.

elasticity (fig 1A,B). Diagnosis: Solid focal lesion in the right breast (BI-RADS 4B). Mammography indicated a high-density mass in the upper outer quadrant of the right breast, approximately 8.1x5.4 cm in size, with clear borders (BI-RADS 4C). Enhanced Magnetic resonance imaging (MRI) scan showed an oval-shaped lesion in the right axillary tail region adjacent to the pectoralis major muscle, with T1W1 low-to-intermediate signal, T2W1 slightly high signal, high signal on diffusion-weighted imaging (DWI), regular morphology, smooth margins, and visible vascular flow voids, with significant peripheral enhancement (fig 1C,D). Diagnosis favored a benign vascular tumor, with the possibility of hemangioma. US-guided biopsy was performed, revealing spindle cell proliferation on pathology examination. The patient underwent surgery, with complete resection of the right breast tumor (fig 1E). Immunohistochemistry results confirmed solitary fibrous tumor: AE1/AE3 (-), p63 (-), CD34 (+), STAT6 (partially +), Bcl-2 (focally +), S-100 (-), SMA, Desmin (-), Ki-67 (+, hot spot 10-15%), CD99 (-), β-Catenin (cytoplasmic +).

Solitary Fibrous Tumor (SFT) is a rare tumor originating from spindle cell mesenchyme. It predominantly occurs in the pleura but can also arise in various other anatomical locations [1]. Histologically, SFT can exhibit various features, ranging from fibrous SFT with few cells, to abundant cells, to malignant-transformed or dedifferentiated SFT with evident sarcomatous changes. Breast SFT occurs across a wide age range from 4 to 70 years [2] presenting as a painless, gradually enlarging mass. Histopathologically, SFT presents as round or oval-shaped lesions composed of short spindle cells and fibroblastic cells. Cells have scant cytoplasm, unclear borders, vesicular nuclei, dispersed chromatin [3]. Immunohistochemically, CD34, CD99, BCL-2, Vimentin, and STAT6 are commonly used markers for diagnosing SFT. Notably, STAT6 is particularly useful in distinguishing SFT from other spindle cell tumor-like lesions. Fibrous lesions of the breast can present with a clinical course ranging from benign to markedly malignant but malignant SFT of the breast are exceedingly rare. Adverse prognostic indicators include large tumor size, positive margins, increased nuclear pleomorphism, vascular invasion, high mitotic index (≥4 mitoses/10 HPF) [4]. For malignant SFT, treatment strategies should include radical resection along with radiation, chemotherapy, and targeted therapy. Given the wide spectrum of spindle cell lesions, ranging from reactive tumor-like conditions to highly malignant sarcomas, accurate diagnosis of SFT is crucial. Diagnosis still relies on histopathological examination and immunohistochemical analysis.

References

1. Ben Ghashir NS, Balalaa NA, Anam W, Mohamed RM. Lipomatous (Fat-Forming) Solitary Fibrous Tumor of the Breast: A Case Report of an Uncommon Variant of a Rare Clinical Entity. Case Rep Oncol 2022;15:455-461.
2. Hwang, US, Kim, SB, Jo, DJ, Kim, SM. Intramedullary solitary fibrous tumor of cervicothoracic spinal cord. J Korean Neurosurg Soc 2014;56:265-268.
3. Salemis, NS. Solitary fibrous tumor of the breast: A case report and the review of the literature. Breast 2017;24:78-81.
4. Nitta, T, Kimura, K, Tominaga, T, et al. Malignant solitary fibrous tumor of the breast. Breast 2021;27:391-393.

Left atrial myxoma adhered to mitral annulus

Xuejie Li[1], Lin Ma[2]

[1]Department of Anesthesiology, West China Hospital, Sichuan University and The Research Units of West China, Chinese Academy of Medical Sciences, [2]Department of Anesthesiology, Shenzhen Children's Hospital, Shenzhen, China

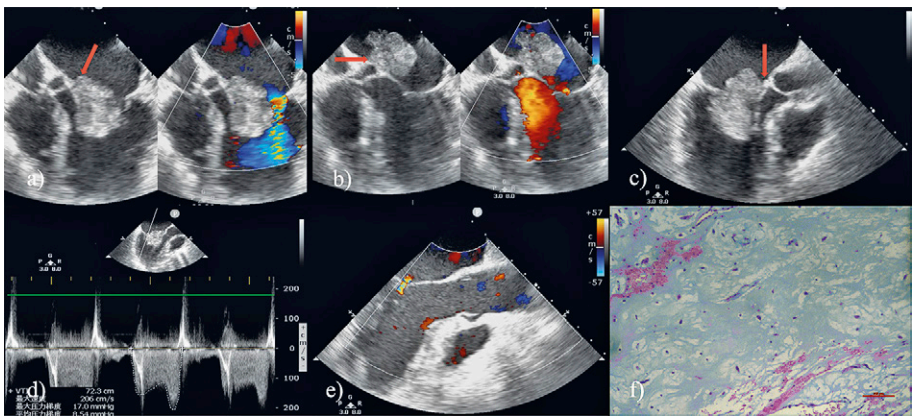

Fig 1. Fig 1. a) The mass caused an acceleration of mitral flow and attached to the mitral annulus; b) the mass protruded completely into the left atrium during systole but did not cause significant mitral regurgitation; c) the long-axis view of the left ventricle also shows that the diastolic mass protrudes into the left ventricle and the mass attached to the mitral annulus; d) Doppler examination showed a maximum flow velocity of 206 cm/s, and the mean pressure difference was 8.54 mmHg; e) the patient underwent laparoscopic mass resection with subtle mitral regurgitation after surgery; f) the postoperative pathological results suggested that the mass was myxoma.

To the Editor,

A 57-year-old man was admitted with recent exertional dyspnea and decreased exercise tolerance. The admitted transthoracic echocardiography showed a mass in the left atrium suspected of being a myxoma. The patient was scheduled for mitral valve replacement and left atrial mass resection under cardiopulmonary bypass. Intraoperative transesophageal echocardiography (TEE) revealed the mass protrudes into the left ventricle during diastole and blocks the mitral valve orifice. The mass caused an acceleration of mitral flow and attached to the mitral annulus (fig 1a). The mass protruded completely into the left atrium during systole but did not cause significant mitral regurgitation (fig 1b). The long-axis view of the left ventricle also shows that the diastolic mass protrudes into the left ventricle and the mass attached to the mitral annulus (fig 1c). Doppler examination showed a maximum flow velocity of 206 cm/s, and the mean pressure difference was 8.54 mmHg (fig 1d). The patient underwent laparoscopic mass resection under cardiopulmonary bypass with subtle mitral regurgitation after surgery (fig 1e). The postoperative pathological results suggested that the mass was myxoma (fig 1f). The patient was successfully discharged from the hospital after seven days, and no recurrence occurred after one year of ultrasound follow-up.

Cardiac myxoma is one of the most common primary cardiac tumors, the majority of which occur in the left atrium [1,2]. Usually, left atrial myxoma arises from the atrial septum at the level of fossa ovalis. If the myxoma is attached to the mitral annulus, the mass can easily block the mitral valve orifice and protrude into the left ventricle. Intraoperative TEE examination can help to identify the attachment point, facilitate surgical decision-making, and real-time evaluation of mitral valve function after op-

Received 12.10.2024 Accepted 27.11.2024
Med Ultrason
2025, Vol. 27, No 1, 109-110, DOI: 10.11152/mu-4483,
Corresponding author: Lin Ma
Department of Anesthesiology,
Shenzhen Children's Hospital, Shenzhen,
Guangdong Province, China
E-mail: malin_0771@163.com

eration. In addition, myxomas that adhere to the annulus, especially the leaflets, may contribute to postoperative mitral insufficiency. It was previously reported myxoma attached to the mitral annulus, valve leaflets, and tendinous cords, and mitral valve replacement was performed after the mass was removed [3]. The difference in our patient was that although the myxoma adhered to the mitral annulus, the removal of the tumor did not affect mitral valve function.

References

1. Yu L, Gu T, Shi E. Echocardiographic Findings and Clinical Correlation With Cardiac Myxoma. JACC Cardiovasc Imaging 2016;9:618-621.
2. Pergolini A, Zampi G, Tinti MD, et al. The Strange Case of the Infarcted Myxoma. Echocardiography 2016;33:476-478.
3. Li XD, Bai Y, Duan XM, Wang XC. A Rare Case of Multiple Myxoma Involving Both Mitral Valve Leaflets. Ann Thorac Cardiovasc Surg 2019;25:117-119.

Torsion with necrosis of a wandering spleen in a child

Xia Li[1], Wenqin Liu[1], Yuting Li[2], Xiaomin Liao[3], Shaozhen Liang[1]

[1]Department of Ultrasound, [2]Department of Radiology, [3]Department of Pathology, The Tenth Affiliated Hospital of Southern Medical University, Dongguan People's Hospital, Dongguan, Guangdong, China

To the Editor,

A 14-month-old girl, with a 3-day history of fever and vomiting, presented to the emergency department with an additional 1-day duration of diarrhea. Upon physical examination, abdominal distension and reduced bowel sounds were evident. Laboratory investigations revealed white blood cell count of 42.62×10^9/L, red blood cell count of 3.47×10^{12}/L, platelet count of 945×10^9/L, routine C-reactive protein level exceeding 200 mg/L, and high-sensitivity C-reactive protein level exceeding 5 mg/L. Abdominal ultrasound indicated an inhomogeneous, oval, and ill-defined mass with a capsule and necrotic areas (fig 1a). Spot-like blood flow signals surrounded the mass, whereas no apparent blood flow signals were noted internally (fig 1b). Abdominal computed tomography (CT) clarified the mass was well-circumscribed and regular, with visible exudation surrounding it (fig 1c). Mild enhancement was pointed out at the margin during the enhanced scan, while the central area showed insignificant enhancement (fig 1d). The girl underwent exploratory laparotomy, revealing a splenic pedicle twisted by approximately 720 degrees, with the spleen turning black and exhibiting a visible pus coating on its surface. Pathological examination subsequently confirmed spleen torsion necrosis, accompanied by significant bleeding and localized microabscess formation. Post-surgery, the

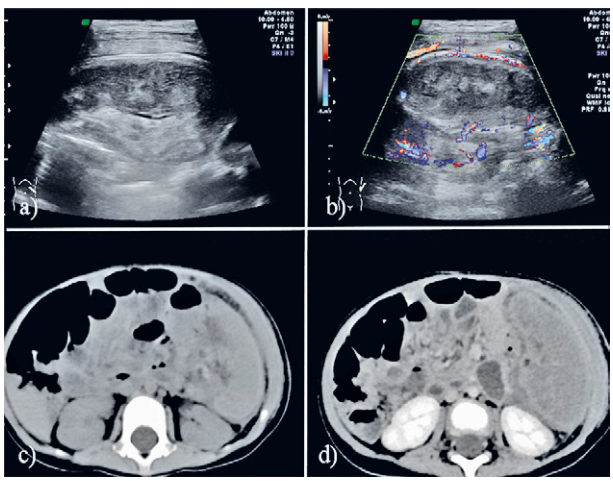

Fig 1. a) Gray ultrasound showed an oval, ill-defined, and inhomogeneous mass with necrotic areas within and a capsule peripherally; b) Color Doppler flow imaging showed no apparent blood flow signals were noted internally and abundant blood flow signals surrounded the mass; c) Plain computed tomography showed the mass was regular and well-defined with visible exudation surrounding it; d) Enhanced computed tomography showed the margin of the mass was mild enhancement and the central area was insignificant enhancement.

Received 05.02.2025 Accepted 10.02.2025
Med Ultrason
2025, Vol. 27, No 1, 110-111, DOI: 10.11152/mu-4484,
Corresponding author: Wenqin Liu, Master of Medicine
Department of Ultrasound,
The Tenth Affiliated Hospital of
Southern Medical University,
Dongguan People's Hospital,
3 Wandao Road South, Wanjiang District,
Dongguan, Guangdong, China
E-mail: liuwenqin6189@163.com

patient experienced secondary thrombocytosis and was managed with dipyridamole therapy.

Splenic infarction in children due to splenic torsion is a rare but severe acute abdominal condition stemming from abnormal splenic positioning, frequently attributed to ligament laxity or congenital anomalies. It predominantly affects children between 3 months and 10 years, with a global incidence below 0.2% [1]. Ultrasound can identify splenic displacement and the "whirlpool sign", indicative of splenic pedicle torsion, albeit with potential limitations due to operator expertise and intestinal gas interference [2]. When ultrasound diagnosis remains uncertain, CT is recommended to delineate splenic position, morphology, size, density alterations, and adjacent organ relationships [3]. Treatment options encompass splenopexy for asymptomatic or mildly symptomatic children to prevent recurrence and splenectomy for those with infarction and worsening symptoms. Following splenectomy, children may be predisposed to risks such as secondary thrombocytosis and thrombosis, necessitating regular follow-up and anticoagulant therapy [4].

References

1. Cui Q, Xu XY, Li C, et al. Wandering spleen combined with pedicle torsion and splenic infarction: a rare case report and literature review. Front Pediatr 2024;12:1429490.
2. Yoshida M, Saida T, Masuoka S, et al. Preoperative diagnosis of a torsioned accessory spleen. J Med Ultrasound 2021;29:116-118.
3. Hamidi H, Osmani H, Zahin RM. Computed tomography features and surgical treatment of wandering spleen torsion: a case report. Radiol Case Rep 2024;19:6213-6216.
4. Wang ZM, Peng CH, Wu DY, et al. Diagnosis and treatment of splenic torsion in children: preoperative thrombocytosis predicts splenic infarction. BMC Pediatr 2022;22:440.

Echocardiography in the rapid detection of postmyocardial infarction complications – a case of giant left ventricle pseudoaneurysm

Mijo Meter[1], Vedran Carević[1], Duška Glavaš[1]

[1]Cardiovascular Diseases Department, University Hospital of Split, Split, Croatia

To the Editor,

A 68-year-old male with a history of arterial hypertension, hyperlipidemia, previous myocardial infarction and ischemic cardiomyopathy was referred to the emergency department due to progressive exercise intolerance and dyspnoea. The physical examination revealed bilateral lung crackles and slight bilateral extremities edema, while laboratory parameters showed increased levels of NT-pro B-type natriuretic peptide. Electrocardiogram demonstrated sinus rhythm with left anterior hemiblock and occurence of Q waves in the inferior leads. The transthoracic echocardiography (TTE), including the 3D TTE, showed a massive left ventricle pseudoaneurysm (LVP) with a narrow neck measuring (6.8x7.9 cm) in the basal part of the inferior wall (fig 1a,b,c). A cardiac magnetic resonance imaging established a partially thrombosed giant LVP of the inferior wall measuring (8.2x8.5 cm) with compression of the left atrium (fig 1d). The patient successfully underwent urgent surgical repair of the LVP with an extracellular matrix patch.

LVP complicating myocardial infarction is a rare complication with an incidence <0.1%. It is surrounded by the pericardial layer or thrombus and carries a substantial risk of rupture if managed medically. Pseudoaneurysms are most often located at the posterior and lateral wall and usually present with symptoms of congestive heart failure, dyspnoea, chest pain and arrhythmias. Myocardial infarction is the most frequent cause, however other causes include infection, chest trauma, and replacement of the aortic or mitral valve [1].

Cardiac imaging modalities, including echocardiography, cardiac computed tomography, and cardiac magnetic resonance play a vital role in precisely localizing the site of rupture, evaluating the number of defects, and

Received 19.01.2025 Accepted 03.02.2025
Med Ultrason
2025, Vol. 27, No 1, 111-112, DOI: 10.11152/mu-4485,
Corresponding author: Mijo Meter
Cardiovascular Diseases Department,
University Hospital of Split,
21000 Split, Croatia
e-mail: mijometer05@gmail.com
Phone: +385 / 98 975-2946

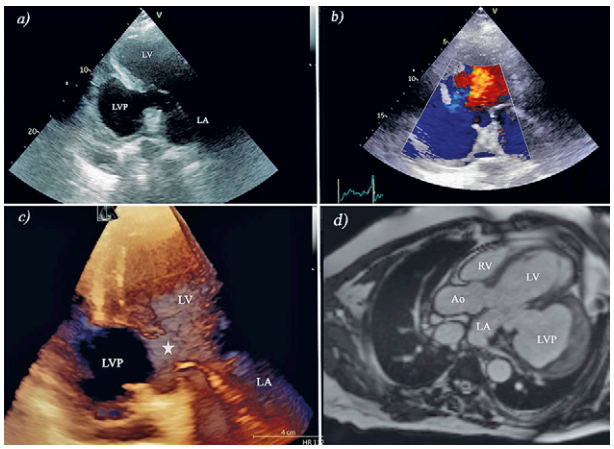

Fig 1. a) TTE showing giant LVP with a narrow neck and wide base in the inferior region of the LV; b) TTE with color Doppler through the cavity of the LVP; c) the 3D TTE demonstrating neck (asterisk) of the LVP and loss of continuity at the basal part of inferior wall; d) cardiac MRI scan of the partially thrombosed LVP with compresion of the left atrium. LA - left atrium, LV - left ventricle, RV - right ventricle, LVP - left ventricle pseudoaneurysm, Ao - Aorta

anatomical relationship with surrounding structures [1]. TTE is a non-invasive and first-line diagnostic modality used in the detection of LVP and other mechanical complications after myocardial infarction. On TTE, LVP is typically shown as an echo-free extracardiac area with a narrow neck and wide base, usually adjacent to the posterolateral wall [2].

Our case emphasizes the important role of echocardiography in the rapid identification of LVP. When in doubt, it is crucial to keep in mind that multimodality imaging is mandatory for the diagnosis of LVP and other sequelae after myocardial infarction.

References

1. Sakaguchi G, Komiya T, Tamura N, Kobayashi T. Surgical treatment for postinfarction left ventricular free wall rupture. Ann Thorac Surg 2008;85:1344-1346.
2. Kupari M, Verkkala K, Maamies T, Härtel G. Value of combined cross sectional and Doppler echocardiography in the detection of left ventricular pseudoaneurysm after mitral valve replacement. Br Heart J 1987;58:52-56

Confusing abdominal pain: images of spontaneous isolated superior mesenteric artery dissection with thrombosis

Shuang Zheng*, Pei Hu*, Xiao-yi Wang, Chao Wang, Xiao-xuan Liu, Zheng-sen Dong, Bin Xiao

** the authors share the first authorship*

Department of Ultrasound, Renmin Hospital, Hubei University of Medicine, Shiyan, China

To the Editor,

A 37-year-old patient complained of intermittent severe abdominal pain, nausea and vomiting for 5 days. He had no history of hypertension or trauma and denied smoking. Common diseases such as urinary calculi, cholecystolithiasis, pancreatitis and myocardial infarction were excluded.

Received 21.11.2024 Accepted 12.12.2024
Med Ultrason
2025, Vol. 27, No 1, 112-113, DOI: 10.11152/mu-4487,
Corresponding author: Bin Xiao MD
Department of Ultrasound, Renmin Hospital,
Hubei University of Medicine,
Shiyan 442000, Hubei, China
E-mail: 7771563@qq.com

Ultrasound revealed that the dilated superior mesenteric artery (SMA) had a diameter of 1.7 cm and an intimal tear located 4 cm away from the opening of SMA and measured 4.5 cm in extent, (fig 1A). Thrombosis was detected in the false lumen, which was separated from the true lumen by the intimal flap. Spectral Doppler showed that the blood flow speed in the true lumen was as high as 141 cm/s, and color Doppler found a blood-filling defect in the false lumen (fig1B,C). Spontaneous isolated superior mesenteric artery dissection (SISMAD) with thrombosis was diagnosed. Transverse and sagittal computed tomography angiography (CTA) images demonstrated a tortuous and dilated SMA with a double-lumen, surrounded by a circular low-density shadow (fig 1D,E). Volume rendering (VR) observed a filling defect in the superior mesenteric artery, with the formation of multiple

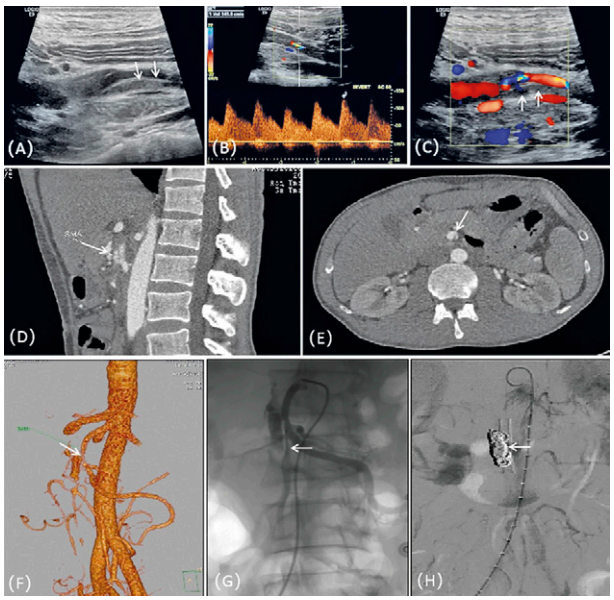

Fig 1. A) Ultrasound revealed an intimal tear (arrows) in the dilated SMA and thrombosis in the false lumen; B,C) Spectral and color Doppler showed that the blood flow speed in the true lumen was as high as 141cm/s, and blood-filling defect in the false lumen (arrow); D,E) Transverse and sagittal CTA images demonstrated a tortuous and dilated superior mesenteric artery with a double-lumen, surrounded by a circular low-density shadow (arrow); F) VR observed a filling defect in the superior mesenteric artery (arrow), with the formation of multiple collateral circulation. G) DSA showed that the true lumen of SMA was compressed (arrow), while the distal SMA was slightly dilated; H) Stent implantation (arrow) was successfully performed.

collateral circulation (fig 1F). The patient's symptoms were not relieved after conservative treatment, so digital subtraction angiography (DSA) and stent implantation were performed. DSA showed that the true lumen of SMA was compressed, while the distal SMA was slightly dilated (fig 1G). The blood flow of SMA and its branches were smooth after stent implantation (fig 1H). The patient recovered well at follow-up.

Secondary causes of SISMAD, a relatively rare vascular disease, include atherosclerosis, cystic medial necrosis, elastic tissue diseases, fibromuscular dysplasia and trauma [1]. Hypertension and smoking are common risk factors, which did not appear in this case. It has been suggested that the mechanism of SISMAD is related to the hemodynamics of SMA. The position of proximal SMA is relatively fixed, whereas the mobility of its distal increases significantly with intestinal peristalsis.[2] The tortuosity of SMA and the difference of mobility can cause the sharp change of local hemodynamic shear, resulting in dissection. The clinical symptoms as well as laboratory examinations of SISMAD are nonspecific, making it commonly misdiagnose and leading to serious consequences [3].

Acknowledgments: The work was supported by Education Department of Hubei (No. B2022132) and Shiyan Science and Technology Bureau of Hubei Province (No. 22Y60).

References

1. Kwon J H, Han Y H, Lee J K. Conservative Management of Spontaneous Isolated Dissection of the Superior Mesenteric Artery. Gastroenterol Res Pract 2017,2017:9623039.
2. Wu X M, Wang T D, Chen M F. Percutaneous endovascular treatment for isolated spontaneous superior mesenteric artery dissection: report of two cases and literature review. Catheter Cardiovasc Interv 2009;73:145-151.
3. Park U J, Kim H T, Cho W H, et al. Clinical course and angiographic changes of spontaneous isolated superior mesenteric artery dissection after conservative treatment. Surg Today 2014,44:2092-2097.

Umbilical artery thrombosis at 38 weeks of gestation

Ziwei Wang, Hong Luo

Sichuan University, West China Second University Hospital, Department of Ultrasound, Key Laboratory of Obstetric and Gynecologic and Pediatric Diseases and Birth Defects of Ministry of Education, Chengdu, China

To the Editor,

A 36-year-old woman (G2P0), presented to the emergency department at 38 weeks and 2 days of gestation with reduced fetal movement. Due to her husband's azoospermia, the pregnancy was achieved through embryo transfer of a 5-day-old blastocyst. She underwent regular prenatal examinations with normal results. At this emergency visit, the fetal heart rate monitoring showed a non-stress test non-responsive type. Prenatal ultrasound (US) examination revealed dense coiling in the umbilical cord with the umbilical coil index of 0.49 (fig 1a). A hyperechogenic filling in the umbilical artery was detected (fig 1b). Color Doppler US demonstrated the absence of blood flow signal in the umbilical artery and only one allantoic artery (fig 1c). The fetal middle cerebral artery (MCA) pulse index was decreased (0.79). Meanwhile, the blood test results of the patients indicated an elevated D-dimer measurement (1.78 mg/L).

Consequently, immediate consent for cesarean section was obtained and resulted in delivery of a girl weighing 2630 g with Apgar scores of 10-10-10 recorded. Postoperative examination confirmed ultrasound findings: the umbilical cord was twisted 17 times, the umbilical cord was purplish red throughout (fig 1d). Histopathological examination demonstrated thrombosis in the umbilical artery. Follow-up evaluations conducted at intervals of one month, six months after birth indicated normal growth.

Received 19.01.2025 Accepted 05.02.2025
Med Ultrason
2025, Vol. 27, No 1, 114-115, DOI: 10.11152/mu-4488,
Corresponding author: Hong Luo, MD, PhD
Department of Ultrasound
West China Second
University Hospital
Sichuan University,
1416 Chenglong Ave,
Chengdu, Sichuan,
China 610066
Phone: +1 18180609092
E-mail: luohongcd1969@126.com

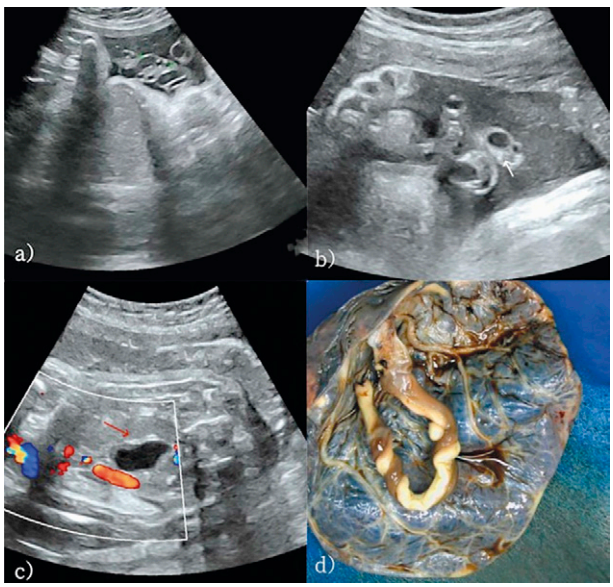

Fig 1. a) Gray scale ultrasound (US) revealed dense coiling with the umbilical coil index of 0.49; b) Gray scale US showed hyperechogenic content of the umbilical artery (white arrow); c) Color Doppler US showed only one allantoic artery is visible in the bladder plane (red arrow); d) A gross specimen of the placenta revealed the umbilical cord was twisted, the umbilical cord is purplish red throughout.

The occurrence of umbilical vessels thrombosis, a rare complication during pregnancy, can result in severe intrauterine distress and fetal demise. The umbilical vein thrombosis is more prevalent compared to umbilical artery thrombosis. The occurrence of arterial clots is associated with a higher likelihood of adverse pregnancy outcomes [1-2]. The possible causes include mechanical damage or abnormal anatomical structure of the umbilical cord, such as entanglement, torsion, excessive length, compression. Additionally, inflammation, abnormal fetal coagulation, maternal glycosuria disease and smoking can also contribute to these conditions [2]. Prenatal ultrasound examination can diagnose umbilical vessels thrombosis. However, due to fetal obstruction, it is difficult to detect umbilical thrombosis prenatally. Therefore, in the presence of high-risk factors and abnormal fetal

movement, it is crucial to meticulously assess parameters such as the degree of umbilical cord coiling, umbilical vessel number and contents, the quantity of allantoic arteries in the bladder plane. Additionally, monitoring indicators like the umbilical artery and middle cerebral artery in fetal holds immense clinical significance for decision-making.

References

1. Sato Y, Benirschke K. Umbilical arterial thrombosis with vascular wall necrosis: clinicopathologic findings of 11 cases. Placenta 2006;27:715-718.
2. Zhu Y, Beejadhursing R, Liu Y. 10 cases of umbilical cord thrombosis in the third trimester. Arch Gynecol Obstet 2021;304:59-64.

The interesting and deceptive intrauterine vesicular lesions: a case of multiple chorionic cysts and its pregnancy outcome

Guilin Ye, Houqing Pang

Department of Ultrasound, West China Second University Hospital, Key Laboratory of Birth Defects and Related Diseases of Women and Children (Sichuan University), Ministry of Education, Chengdu, Sichuan, China

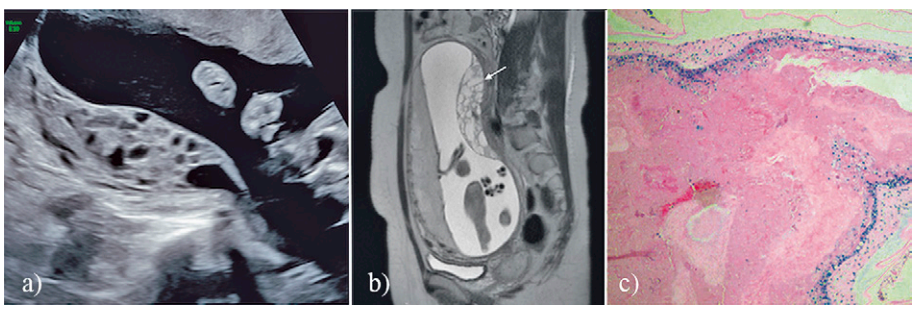

Fig 1. a) Ultrasound showed honeycomb cystic lesions on the fetal membranes; b) MRI illustrated a mixed signal mass with a clear boundary from the myometrium (arrow); c) HE staining of the chorionic cyst and fibrin deposition inside

To the Editor,

A 30-year-old woman (G3P0+2) conceived after two fertilized frozen embryos were transferred through in vitro fertilization. Ultrasound during early pregnancy showed a single live fetus and no major anomaly was detected. At 22 weeks, the routine ultrasonographic examination showed a honeycomb-shaped lesion measuring 8.3x2.1x8.4 cm on the right posterior upper wall of the uterus away from the placenta (fig 1a). The serum β-hCG concentration was greater than 200,000 mIU/ml. The patient was subsequently included in a multidisciplinary consultation. Thoracic and abdominal MRI and amniocentesis were performed. MRI showed that the tumor had no local infiltration or distant metastasis (fig 1b), and the chromosomes of the fetus were normal. Based on the above findings, partial chorionic edema was suspected. After intensive counseling of potential risk, pregnancy was decided to be continued with close feto-maternal surveillance and serial β-hCG monitoring. The serum β-hCG was 168960.8mIU/ml at 25 weeks and declined progressively thereafter. Similarly, the cystic lesions did not grow. There were no complaints during pregnancy.

The patient underwent cesarean section at 39 weeks and delivered a live infant. The fetal membrane and placenta were intact, and rotten vesicular tissue was visible on the free fetal membrane. Histopathology revealed a large amount of fibrinoid deposits with trophoblastic

Received 12.12.2024 Accepted 03.02.2025
Med Ultrason
2025, Vol. 27, No 1, 115-116, DOI: 10.11152/mu-4481,
Corresponding author: Houqing Pang
Department of Ultrasound,
West China Second University Hospital,
20, Renmin Road South,
610041, Chengdu, China
E-mail: panghouqing75@163.com

proliferation in the lesions (fig 1c), with markers P57(+) and Ki67 <10%. Short tandem repeat (STR) genotyping showed that the pregnancy tissue was biparentally diploid, ruling out the diagnosis of hydatidiform mole. A diagnosis of multiple chorionic cysts was made. At follow-up examination, serum total hCG levels showed an increase weekly. Chest and abdominal CT demonstrated multiple uterine and lung metastases. The patient received single-dose dactinomycin chemotherapy. At the end of chemotherapy, the pulmonary lesions had become undetectable, and the serum hCG dropped to normal levels without recurrence.

Most chorionic cysts are located on the placental surface and bulge into the amniotic cavity [1]. This is the first report of multiple chorionic cysts at the free fetal membrane. We speculate that the incomplete degeneration and hypoxia of the smooth chorionic villi and the deposition of surrounding fibrin fluid are the causes of chorionic cysts [2]. It is worth noting that when imaging examination reveals a vesicular mass in the uterine cavity during pregnancy, it is particularly important to distinguish whether it is located inside or at the edge of the placenta, or far away from the placenta, because the former is a common manifestation of hydatidiform mole or placental mesenchymal dysplasia. In addition, the serial β-hCG level detection and chromosome karyotype analysis can help clarify the cause and formulate a pregnancy plan. However, the relationship between multiple chorionic cysts and postpartum gestational trophoblastic neoplasia remains to be elucidated.

References

1. Brown, DL, DiSalvo, DN, Frates, MC, et al. Placental surface cysts detected on sonography: histologic and clinical correlation. J Ultras Med 2002;21:641-646; quiz 647-648.
2. Bonasoni, MP, Comitini, G, Blasi, I, et al. Large Subchorionic Cyst Located at Umbilical Cord Insertion with Vascular Displacing and Intracystic Hemorrhage/Hematoma: A Case Report. Fetal Pediatr Pathol 2020;41:468-474.